Heliyon 5 (2019) e02595

Contents lists available at ScienceDirect

Heliyon

journal homepage: www.heliyon.com

Research article

The effect of graphite intercalated compound particle size and exfoliation temperature on porosity and macromolecular diffusion in expanded graphite

R. Goudarzi, G. Hashemi Motlagh *

Advanced Polymer Materials & Processing Lab, School of Chemical Engineering, College of Engineering, University of Tehran, 16th Azar Ave, Enqelab St, P.O.Box: 11155-4563, Tehran, Iran

ARTICLE INFO

Keywords:
Materials science
Nanotechnology
Nanomaterials
Materials application
Materials characterization
Materials property
Materials structure
Expanded graphite
Nanographite
Microstructure
Porosity
Exfoliation temperature
Diffusion
Adsorption
Oil

ABSTRACT

The pore structure of expanded graphite (EG) including pore volume, pore size distribution and surface area is investigated by mercury porosimetry, nitrogen adsorption and SEM. Also, the diffusion of silicone oil molecules as macromolecules with different molecular weights into EG pores is studied. Various EG samples were prepared by the sudden heating of graphite intercalated compound (GIC) with varying particle size of 35, 50, 80 and 200 meshes in an electrical furnace at temperatures of 700, 800 and 900 °C. The EGs were characterized by FTIR to evaluate the presence of functional groups. It was found that the exfoliation process has not significantly introduced oxygen functional groups such as epoxy and carboxyl groups to the EG structure. Therefore the chemical structure of the EG is very close to pristine graphite. The mercury porosimetry results showed a broad range of total pore area from 5 to 31 m^2/g for the EGs. The particle size of GIC and exfoliation temperature showed strong effects on the pore size of EG. The mercury intrusion porosimetry and nitrogen adsorption isotherms revealed that μm-pores are dominant as compared with nm-pores in all EG samples. The diffusion of silicone oils as macromolecular guests with three different viscosities was experimentally studied to analyze the diffusion facts of EG as the host. It was observed that as the exfoliation temperature decreases, the sorption capacity decreases; and EG samples prepared from the GICs with smaller particle size have lower sorption capacity. Sorption experiments also showed that the whole pore volume of EG is not filled with silicone oil leading to this fact that EG includes relatively closed pores. A new model was suggested for the sorption capacity of EG as a function of the pore area of EG and the square root of molecular weight of silicone oil.

1. Introduction

For the efficient utilization of graphite as filler in polymer matrices, its stacked graphene layers must be separated into nanosheets. Broadly, three treatment methods are adopted to obtain modified graphite forms termed as graphene oxide, graphite intercalated compound (GIC) and expanded graphite (EG) [1]. The types of nanographite materials have developed significantly due to the coexistence of different superior properties and numerous innovative synthesis methods [2]. EG is a highly prospective nanographite material due to its unique properties including very low density, high aspect ratio, high porous structure, closest electrical/thermal conductivity and thermal/chemical stability to natural graphite and ease of preparation and low cost. EG is exceptionally a useful nanomaterial to make polymer composites for various applications such as conductive polymer parts, heat resistance parts, sealing gaskets and flame retardant polymer composites. Generally, EG is obtained by rapid heating of GIC. GICs are prepared by the reaction of intercalation compounds such as strong acids with graphite [3]. The acid molecules penetrate between graphite layers and then applying a thermal shock in an electrical furnace causes a rapid vaporization of the intercalated species; the force caused by the exhaust of these gaseous products exfoliates the graphite layers and consequently a significant increase in volume takes place and EG with very low density is obtained. The surface area of graphite significantly increases during the exfoliation process owing to the formation of abundant pores, resulting in favorable adsorption properties [4]. EG has been widely used in waste gas removal, removal of petroleum from water surface [5], catalyst carrier [6], medical materials [7] and many other fields [8, 9] in which adsorption is a

* Corresponding author.
E-mail address: ghmotlagh@ut.ac.ir (G. Hashemi Motlagh).

https://doi.org/10.1016/j.heliyon.2019.e02595
Received 2 May 2019; Received in revised form 7 August 2019; Accepted 1 October 2019

key property. Inagaki et al [10] showed that an EG with a low bulk density of 0.007 g/cc can adsorb more than 80 g of an A-grade heavy oil, which is considerably higher than the sorption capacity of conventional sorbents of heavy oils.

Many researchers have investigated the preparation methods of EG. Various exfoliation conditions i.e. temperature and heating time have been studied in the preparation of EG from GIC with the aim of achieving highest surface area or lowest bulk density. Overall, a temperature of 900 °C and a heating time of 5–30 s have been found as the optimum condition to prepare EG with a bulk density of 0.003–0.02 g/cc and aspect ratio of 200–1500 [11]. Liu et al [3] reported that EG can be produced in one-step method at room temperature through intercalation with concentrated sulfuric acid and ammonium persulfate. The prepared EG expanded to the specific volume of 225 ml/g. Bonnissel et al [12] suggested a model to calculatethe change in thermal conductivity and permeability versus bulk density of EGs prepared at varying exfoliation temperatures of 300–1000 °C from GIC. By increasing the exfoliation temperature, the apparent density of EG decreased. Afanasov et al [13] prepared EG in air at various temperatures of 250, 400, 600, 900 °C from oxidized graphite. They observed that increasing exfoliation temperature from 200 to 600 °C increased the specific surface area of the prepared EG up to a maximum value of 150 m^2/g. But the exfoliation temperature of 900 °C, significantly reduced the specific surface area because of the burning of graphite oxide in air at such a high temperature. In another work they [14] synthesized EG from graphite nitrate obtained by the oxidation of anodic graphite in 58% aqueous nitric acid solution. They expanded GIC at exfoliation temperatures of 900 °C and 600 °C in air and obtained EGs with specific surface areas of 20 m^2/g and 150 m^2/g, respectively.

The influences of various oxidizing agents, their concentrations and ratios on GIC preparation have been investigated. Inagaki et al [15] suggested that the oxidation of graphite is limited by chemical oxidation depending on the oxidizer. The concentration of sulfuric acid affects the upper limit of saturated potential. Teplykh et al [4] determined the crystal structure of the main phase of EG samples prepared by rapid thermal decomposition of intercalation compounds of graphite aminofluoride, oxidized graphite and graphite fluoride using neutron diffraction and X-ray diffraction analysis. Hristea et al [16] prepared EG by suspending graphite in a mixture of H_2SO_4 and HNO_3. Then oxidizing agents such as $KMnO_4$ or $FeCl_3$ were added. Increasing the molar ratio of H_2SO_4 to HNO_3, 1:1, 4:1 and 9:1 for GIC preparation, caused reductions in the surface area of EG from 158 to 90 m^2/g. $KMnO_4$ showed a more oxidizing effect than $FeCl_3$ due to a higher degree of graphite oxidation and consequently exfoliation ratio and surface area.

Tao et al [17] used microwave heating instead of electrical furnace to expand GIC. They found that the original structure of graphite was unchanged by the microwave irradiation; however, its crystallinity decreased significantly. The resulting EG had a worm shape structure with abundant pore networks and a specific surface area of 54 m^2/g, similar to the EG specimens prepared by electrical furnace. Using microwave radiation for production of EG also reported by Sridhar et al [18].

Few works have reported the effects of GIC size on the properties of resulting EG. Dhakate et al [19] investigated the effects of EG particle size on the mechanical and electrical properties of epoxy/EG composites. GICs with 30, 50, 150, and 300 μm were employed. They observed that composites containing EG prepared from 300 μm GIC give high electrical conductivity. On the other hand, composites containing EG prepared from 30 μm GIC give high mechanical properties and low electrical conductivity. The composites containing EG with mixed size of GIC showed the desired mechanical and electrical properties.

EG is also an effective material to make polymer composites for various applications such as conductive polymer parts used in fuel cell elements and capacitors, heat resistance parts, sealing gaskets and flame retardant polymer composites. Many researchers have studied the preparation and properties of polymer/EG composites [20, 21, 22]. Yasmin et al [11] fabricated EG polymer nanocomposites with 1–2 %wt. of EG by direct, sonication, shear, and a combination of sonication and shear mixing. The results showed the combination of sonication and shear mixing provided the optimum elastic modulus and tensile strength, whereas the lowest results were obtained by the direct mixing technique. The EG composites are also prepared using a compressed EG sheet which is impregnated with the resin and cured [23]. The EG composites exhibited a sharp transition from an electrical insulator to an electrical semiconductor at a low EG content of about 1.0 %wt. This is due to the worm-like structure of EG particles having a high aspect ratio. Such filler geometry enables the formation of conducting networks in polymer matrices at lower filler contents. But EG decreased the mechanical properties of the thermoset resin matrix, due to the existence of abundant pores in EG [11, 24]. Similar to layered silicates, only some polymer chains can be diffused into the galleries or the multipores of EG [23].

The properties and structure of EG has been investigated by few studies through mercury porosimetry, nitrogen adsorption [25] and electron microscopy [26]. Hoang et al [27] prepared EG by the mixing of natural graphite with $KMnO_4$, $HClO_4$ and $(CH_3CO)_2O$ at weight ratios of 1:0.5:1:0.4 for 10 s. Then, EG was prepared by 2.45 GHz microwave irradiation at 720 W and for 40 s. Through N_2 adsorption/desorption analysis they reported a total pore volume and surface area of 0.046 cm^3/g and 30 m^2/g for the prepared EG while those of natural graphite were 0.007 cm^3/g and 3 m^2/g, respectively. For a commercial EG a total pore volume of 23 cm^3/g measured by mercury porosimetery was reported by Toyoda et al [5]. Another EG material with BJH mean pore diameter of 26 nm and surface area of 24 m^2/g possessed a reasonable amount of macropores (greater than 50 nm), small fraction of mesopores (2–50 nm) and few micropores (less than 2 nm). The pores larger than 300 nm were ignored [28].

The properties of EG/polymer composites are dependent on EG structure, so it is very useful to have more insight into the pore structure of EG. Numerous works have studied the diffusion of graphite [29, 30], EG synthesis and the properties of EG/polymer composites and there are some reports on the structure and porosity of EG but complete characterization of EG including pore size distribution, average pore diameter as well as the filling percentage of the multipores by a macromolecule or oligomer, needs more attention. Therefore, in the present work, efforts are taken to study the porosity characteristics of EG and the diffusion process of varying length oligomers (silicone oil) into EG. The influence of GIC particle size and exfoliation temperature on porosity characteristics and oil sorption is also considered. A new model has been proposed for the oil sorption of EG as a function of oil molecular weight and EG pore area.

2. Material and methods

2.1. Materials

A graphite intercalated compound (GIC) with an average particle size of 500 μm (35 mesh), >95wt% carbon, exfoliation ratio of 250 and moisture content <1wt% supplied by China Superior Graphite, was used as received to prepare expanded graphite. Silicone oil in three viscosities 100 cSt, 350 cSt and 1000 cSt was supplied by KCC corporation, South Korea.

2.2. Preparation

In order to prepare EG with various particle sizes, the original 35 mesh GIC powder was milled in a ring mill in small amounts of about 1 g in consecutive steps of 30 s to obtain milled powder with adequate small particle size. The milling was carried out in short sequences to avoid high temperature rise during milling. Then the milled powder was sieved and classified in a stainless steel sieve shaker including sieves of 50, 80 and 200 meshes.

To prepare expanded graphite, the GIC powders were heated in an

electrical furnace at 700–900 °C for 30 s where a huge exfoliation of up to 250 times was occurred. Then the obtained EG was immediately removed from the furnace and kept in the lab to cool down.

According to Table 1 six types of EG were prepared with varying either exfoliation temperature or GIC particle size. The exfoliation time was 30 s for all the prepared EGs.

2.3. Analysis

The microstructure of EG particles was investigated by scanning electron microscopy (SEM), KYKY EM3200 (China) at 30 kV to observe the appearance, shape and size of the pores as well as the thickness of the graphitic nanolayers.

The functional groups of EG was characterized by Fourier transform infrared spectroscopy (FTIR), BRUKER Tensor 27 (Germany), in the range of 4,000–400 cm^{-1} and using a KBr matrix.

Mercury intrusion porosimetry, Micromeritics Instrument Corporation (USA) from pressure of 0.10–60000 psia was used to investigate the pore structure of EG based on Washburn's equation.

The volume of multipores was deduced from nitrogen adsorption isotherms obtained from a porosity analyzer PHS-1020 (PHS, China) at 77 K and the outgas temperature of 250 °C. The surface area was estimated by applying Brunauer, Emmett, and Teller method (BET method) which is an extension of the Langmuir model of monolayer adsorption to multilayer adsorption.

The bulk density of EG was determined by measuring the mass and apparent volume of an EG sample. The volume was measured where EG was poured into a volumetric flask without compaction.

Silicone oil was used for the sorption experiments, according to the steps shown in Fig. 1. First silicone oil was added to a 0.02 g sample of EG powder and the mixture was left for a few seconds. The oil sorption took place very fast in less than a second and complete saturation was achieved. Gulnura et al [31] also reported that the majority of oil sorption by EG occurs in the first moments. Then the unsorbed oil i.e. excess oil was removed by placing the oil-EG mixture on a filter paper for 24 h. After that the oil saturated EG was picked up and weighed to determine the amount of adsorbed oil and calculate the specific sorption. This technique has been used in previous studies for measuring heavy oil sorption of EG, however without investigating the pore size distribution of EG [16, 32].

3. Results and discussion

3.1. Scanning electron microscopy (SEM)

The loose and porous structure of the EG samples prepared at three exfoliation temperatures of 900 (EG1), 800 (EG2) and 700 °C (EG3) for 30 s from 35 mesh GIC are shown by SEM micrographs in Fig. 2. The worm-shape with loose and porous structure of EG have been also reported in previous works [32, 33, 34]. It is comparatively seen that with decreasing the exfoliation temperature, the exfoliation volume decreases.

The SEM images of EG specimens prepared from GICs with 50 (EG4), 80 (EG5) and 200 (EG6) mesh particle sizes, exfoliation temperature of 900 °C and exfoliation time of 30 s, are shown in Fig. 3. Smaller the GIC size, much shorter in length is the accordions of the prepared EG. This

Table 1
EG samples prepared from GIC with varying particle size at different exfoliation temperatures.

EG code	Exfoliation temperature (°C)	GIC mesh	GIC average particle size (μm)
EG1	900	35	500
EG2	800	35	500
EG3	700	35	500
EG4	900	50	297
EG5	900	80	177
EG6	900	200	74

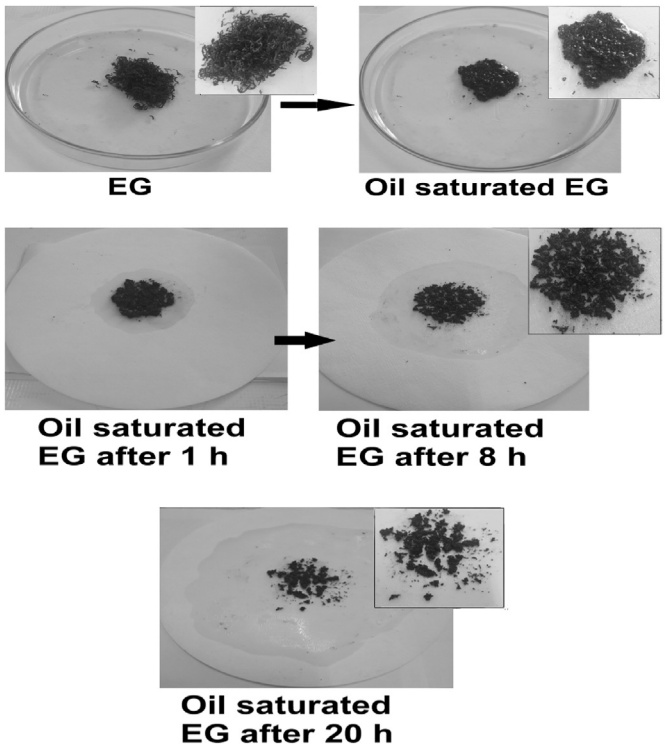

Fig. 1. Oil sorption test procedure for EG.

means that the number of the exfoliated layers in one GIC particle decreases when GIC particle size decreases. Therefore lower exfoliation is seen for the smaller GIC. Dhakate et al [19] also observed that with decreasing particle size of natural graphite, the exfoliation ratio of the resulting EG decreases.

3.2. FTIR analysis

Fig. 4 shows the FTIR spectra of EG specimens prepared at the three different exfoliation temperatures. The band at 3415 cm^{-1} is attributed to O–H stretching vibrations of phenolic or alcoholic functional groups presented on the EG or O–H of adsorbed water which is usually with graphite even if dried [19, 35]. The presence of carboxyl functional groups can also be detected at around 1620 cm^{-1} [28]. It is seen that the exfoliation temperature does not significantly affect the functional groups on EG. Also the increase in the exfoliation temperature from 700 °C to 900 °C has not led to a significant degradation of SP2 carbon structure of EG; The peak at 1460 cm-1 is of the C–C–C symmetric stretching vibration [19].

3.3. Analysis of pore structure

EG is usually used to make polymer nanocomposites where its sorption properties are very dependent on its pore microstructure. In this part the pore structure of EG specimens has been investigated by visual comparison, mercury porosimetry and nitrogen adsorption. The relative amount of macropores (>50nm), mesopores (2–50 nm) and micropores (<2nm) is a key question. The effect of GIC particle size and exfoliation temperature on pore volume, pore area and pore size is presented.

The comparative apparent densities of EG specimens are shown in Fig. 5 where the weights of the three samples are the same. They show lower apparent density for the EG prepared at higher exfoliation temperature. This is due to the higher exfoliation of graphite layers by the higher exfoliation force of the released intercalation volatiles at higher exfoliation temperature. The lowest bulk density for EG prepared in this work is 0.0038 g/cc equivalent to an exfoliation ratio of about 295 for the

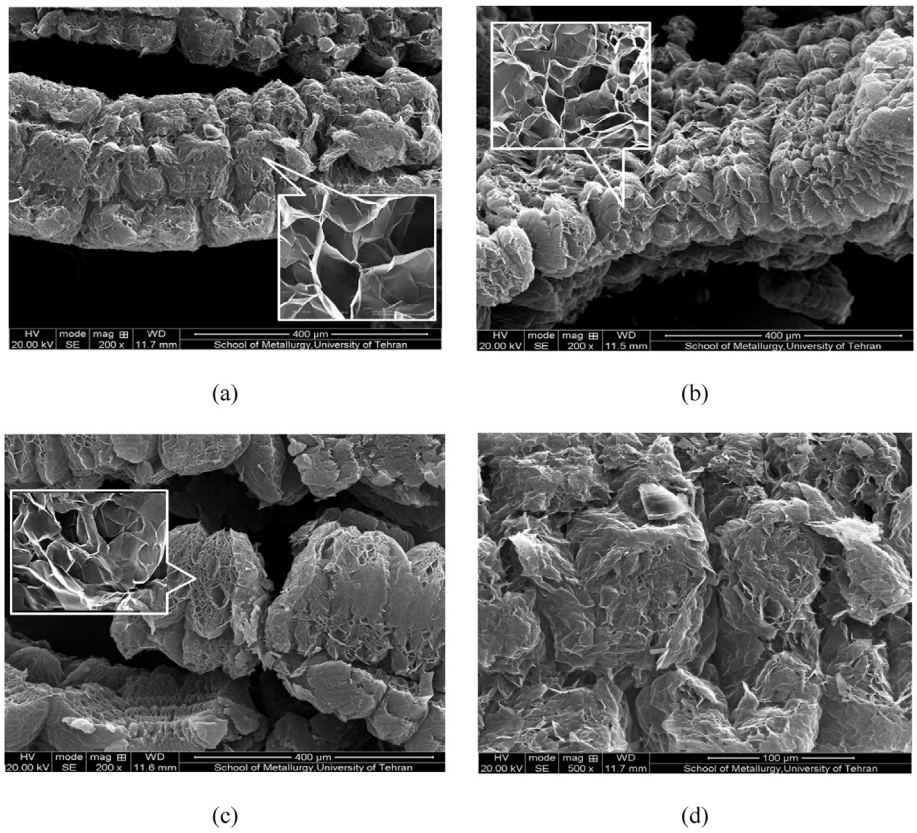

Fig. 2. SEM micrographs of EG specimens prepared at varying exfoliation temperatures, (a) EG1 (900 °C), (b) EG2 (800 °C), (c) EG3 (700 °C), (d) EG3, at higher magnification.

35 mesh GIC expanded at 900 °C for 30 s (EG1). Afanasov et al [14] reported similar results with a bulk density of 0.0025 g/cc for the EG prepared at 900 °C. They also observed that by increasing the exfoliation temperature, the apparent density of EG decreases [12].

Fig. 6 shows the volume of EG specimens with the same weight but prepared from three different GIC mean particle size of 50, 80 and 200 meshes. It is seen that larger particle size GIC results in EG with higher volume, exfoliation ratio and lower apparent density. For the smaller GIC particles, the length scale for the volatiles to escape is shorter and therefore gas pressure could be lower and time to release the gas becomes shorter and consequently lower exfoliation takes place.

By comparing Figs. 5 and 6 it can be realized that the effect of GIC particle size on the bulk density of EG is more pronounced than the effect of exfoliation temperature.

The measured bulk density of the prepared EGs is given in Table 2 ranging from 0.0038 to 0.0552 g/cc. It is seen that higher are the exfoliation temperature and GIC particles size lower is the bulk density of EG. From these bulk density values the nominal pore volume of the EGs are also calculated and presented in Table 2. They are in a broad range from 17 to 262 cc/g. As seen the total pore volume of the EGs prepared from GIC/35mesh is much larger than that for the EGs prepared from smaller GIC particles.

Mercury intrusion porosimetry was employed to investigate the pore structure of the EG samples. The results are shown in Table 2 showing a wide range of 5–31 m^2/g for the total pore area of the prepared EGs. It is seen that increasing the exfoliation temperature from 700 to 900 °C (EG3, EG2, EG1) leads to an increase in the total pore area, which is due to the larger exfoliation of GIC at higher exfoliation temperature. Afanasov et al. also found that raising the exfoliation temperature from 200 to 600 °C increases the specific surface area of the EG from 5 to 150 m^2/g [13]. As shown in Table 2, increasing GIC particle size causes a significant drop in the specific pore area of the prepared EG. According to Table 2 the effect of GIC particle size on the surface area of the resultant EG is stronger than the effect of exfoliation temperature.

There is a large difference between the pore volume values derived from bulk density and measured by mercury porosimetry. This is probably due to the presence of closed pores or very tiny pores which mercury cannot penetrate.

The pore size distribution was also characterized by mercury porosimetry. As seen in Fig. 7, the pore sizes of the EG specimens are in the 0.1–100 µm range i.e. µm-pores are dominant while the pores smaller than 100 nm are not detected by mercury porosimetry. Tao et al [17] also reported by mercury intrusion porosimetry that pores of EG are dominant in 0.1–10 µm range.

In Fig. 7 the specific pore volume (ml/g) increases with increasing exfoliation temperature; also the peaks shift to higher pore diameter. It shows that the number of pores with large diameters increases for the EG specimens prepared at higher exfoliation temperatures. In Fig. 8 similar trend is observed for EG specimens prepared from GICs with varying size. Higher pore volume and larger pore diameter is observed for larger GIC. Again it is seen than the effect of GIC particle size is more significant than exfoliation temperature.

Since pores smaller than 100nm were not detected by mercury porosimetry, low-pressure nitrogen gas adsorption-desorption was employed to further investigate the pore structure of the EGs. Subcritical N_2-gas adsorption techniques are best suited for investigation of materials with fine pores in the range from about 2–300 nm [36]. The results are shown in Fig. 9 for EG4 and EG6. As seen the total pore volume of EG6 is much lower than EG4 confirming the mercury porosimetry observations for the fact that smaller is the GIC particle size, lower is the porosity

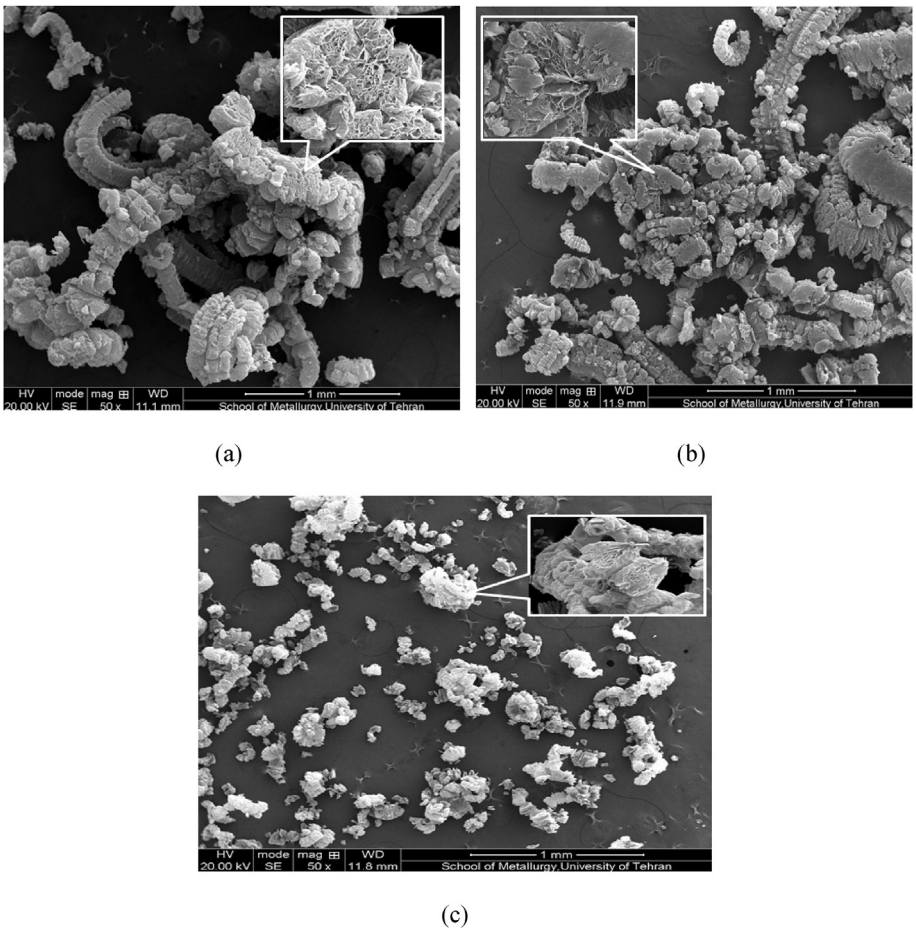

Fig. 3. SEM micrographs of EG specimens prepared from GIC of varying particle size at an exfoliation temperature of 900 °C, (a) EG4 (mesh 50), (b) EG5 (mesh 80), (c) EG6 (mesh 200).

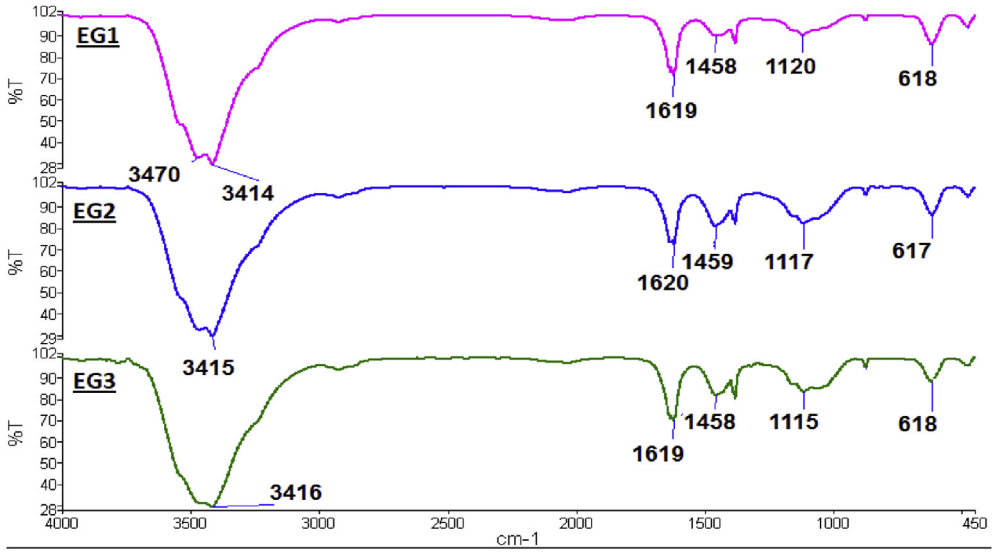

Fig. 4. FTIR spectra of EG specimens prepared at three different exfoliation temperatures of EG1 (900 °C), EG2 (800 °C) and EG3 (700 °C).

of the resulting EG. The adsorption and desorption branches (Fig. 9, a) follow the same path i.e., there is no significant hysteresis. The observed adsorption-desorption isotherms correspond to the typical type II isotherms (IUPAC, 1985), suggesting the existence of macropores. The type II isotherm is an indication of the formation of an adsorbed layer, whose thickness increases progressively with increasing relative pressure as P/P_0 [36]. The type II isotherms for EG have also been previously reported [28, 32]. The inflection point occurs near the completion of monolayer coverage and the beginning of multilayer sorption. The established methods for the determination of pore sizes in Fig. 9, b, are based on

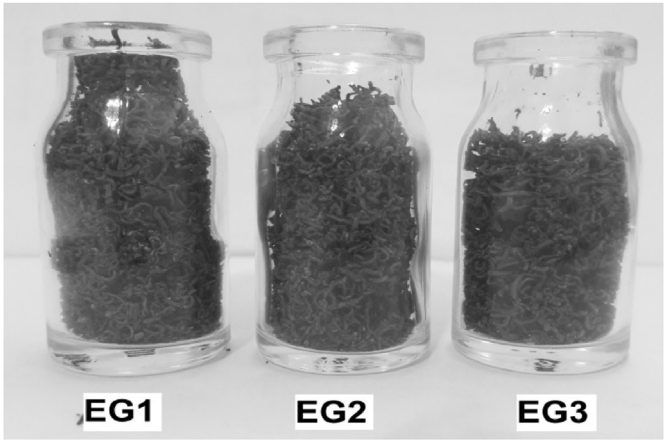

Fig. 5. The qualitative comparison of bulk density for the EGs prepared from GICs at varying exfoliation temperatures of 700 °C (EG3), 800 °C (EG2) and 900 °C (EG1).

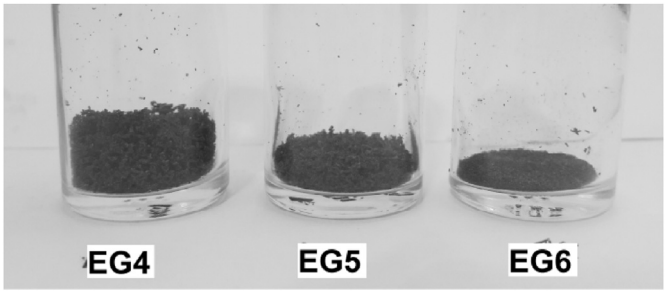

Fig. 6. The qualitative comparison of the EG samples, for bulk density, prepared from. GICs with different particle sizes of 50 (EG4), 80 (EG5) and 200 (EG6) mesh.

Kelvin model or its variance such as Barrett Joyner and Halenda (BJH) [37] method. The BJH method is the most widely method for the analysis of nitrogen adsorption/desorption results [37]. Fig. 9, b does not indicate significant peaks for mesopores or micropores.

The pore volume and the surface area derived from nitrogen adsorption/desorption analysis are listed in Table 3. As seen the nitrogen based pore area is close to the mecrcury based pore area since the specific area is mainly determined by the presence of mesopores and micropores i.e. smaller tiny pores have big influence on specific pre area. But the nitrogen based pore volume of the mesopores and micropores is much smaller than the total pore volume measured by mercury porosimetry. This suggests that the EGs prepared in this work contain a significant amount of macropores (greater than 50 nm, specially 100 nm to 100 μm), small fraction of mesopores (2–50 nm) and rare micropores (less than 2 nm) which is in agreement with previous studies [28, 32]. Having said that for EGs with very high pore area e.g. >150 m^2/g the share of mesopores and micropores increases significantly [13].

3.4. Silicone oil sorption

The sorption of silicone oil with three different viscosities in EG specimens was carried out at room temperature. It was found that all EG samples adsorb silicone oil at room temperature, very quickly, within few seconds. Silicone oils, polydimethylsiloxanes, with various viscosities of 100cSt, 350cSt and 1000cSt and accordingly various molecular weight and length scale [38] as given in Table 4 were used. The diffusion of silicone with varying molecular weight into EG structure was investigated. The used silicone oils have relatively monodisperse molecular weight distribution and therefore the effect of chain length on diffusion into EG galleries can be evaluated.

The oil sorption capacities of EG specimens, at different exfoliation temperatures are shown in Fig. 10. It is seen that as the exfoliation temperature increases, from 700 °C to 900 °C, the sorption capacity of EG increases which is due to the higher porosity in EG prepared at higher exfoliation temperature. The silicone oil with lower viscosity penetrates at higher amount into the pores of EG. This means that EG specimens have pore size distribution where large molecules cannot diffuse into the smaller pores. Comparatively it is worth mentioning that high molecular weight silicone oil cannot penetrate into EG galleries and oil sorption is much lower for EG specimens prepared at 700 °C and 800 °C exfoliation temperatures. Furthermore the trend for silicone oils with viscosities of 100 and 350 are similar.

Fig. 11 illustrates the silicone oil sorption capacity of EG prepared at 900 °C with different average particle sizes of GIC. As seen, the sorption capacity and trend of the oils 350 cSt and 1000 cSt is similar. The silicone oils with higher molecular weights (350 cSt and 1000 cSt) appear to have failed to enter EG pores. In addition, the increase in the average particle size of GIC has no particular effect on the sorption capacity of EG with 350 cSt and 1000 cSt oils. But for silicone oil 100 cSt, there is a significant drop (about – 76%) in the sorption capacity of EG with a decrease in the particle size of GIC from mesh 50 (EG4) to mesh 80 (EG5). Therefore it can be concluded that the porosity of EG is close to the size of silicon oil 100 cSt. The porosimetry results also showed that the pore size distribution of EG is in the 0.1–100 micron range which matches the hydraulic volume of the 100 cSt silicon oil chains.

Table 5 shows the percentage of filled pores of EG specimens with silicone oils. The percentage of filled pores of EG is estimated by calculating the volume of absorbed oil to the EG total pore volume in Table 2 calculated from bulk density. It is seen that only less than 30% of the EG pores are accessible by a resin, such as silicone oil. The percentage of filled pores decreases with increasing silicone oil viscosity, which could be an important fact to be considered in the production of EG nanocomposites. Also for EG specimens with higher porosity or lower bulk density, higher oil filling is observed. However the higher oil filling for EG6 especially for oil 1000 cSt can be due to the increase in the external contact surface of EG particles and an error due to the trapping of such heavy oil in the outer space between the EG particles.

The partial filling of the pores with silicone oil chains of nanometer length suggests two possibilities. First some of the pores are closed spaces that oil cannot penetrate. Second possibility is the presence of nanopores smaller than 100 nm in the structure. But they were not detected by

Table 2
The properties of the prepared EGs from varying size GIC particles at different exfoliation temperatures.

GIC size	35 mesh			50 mesh	80 mesh	200 mesh
Exfoliation temperature	900 °C	800 °C	700 °C	900 °C		
Property	EG1	EG2	EG3	EG4	EG5	EG6
Bulk density (g/ml)	0.0038 ± 0.0002	0.0044 ± 0.0001	0.0049 ± 0.0001	0.0094 ± 0.0002	0.0166 ± 0.0002	0.0552 ± 0.0003
Equivalent pore volume* (ml/g)	262	226	203	105	59	17
Total pore area** (m^2/g)	31	28	25	27	13	5
Total pore volume** (ml/g)	43	40	35	38	28	5

* Calculated from bulk density.
** Obtained from mercury porosimetry.

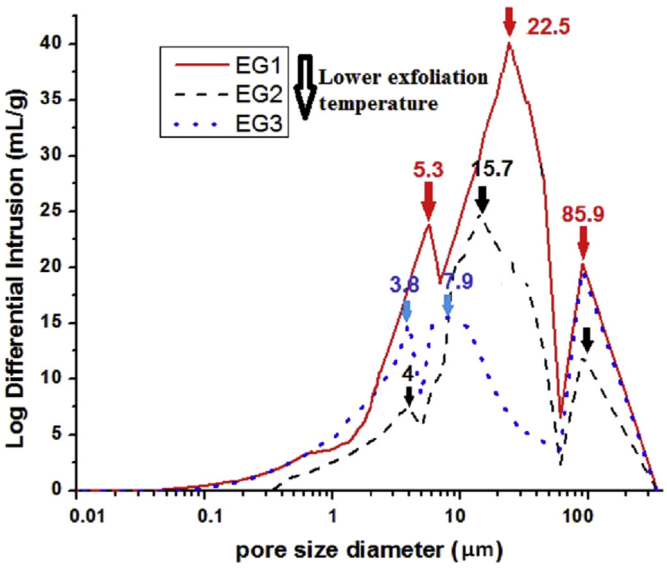

Fig. 7. The pore-size distribution of the EGs prepared at different exfoliation temperatures.

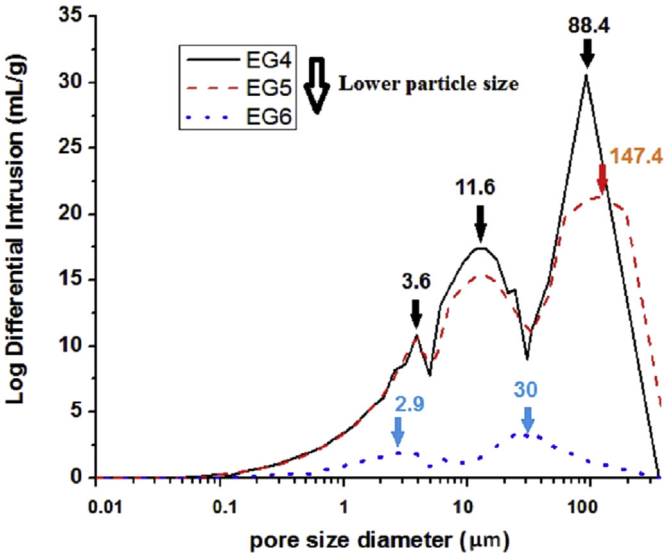

Fig. 8. The pore-size distribution of the EG specimens prepared from varying size GICs.

nitrogen adsorption. Therefore the partial filling is mostly due to the closed pores. This is in agreement with the difference between the pore volume values of Table 2.

To verify the experimental values obtained in the experimental part some theoretical and mathematical calculations can be considered. Since hypothetical monolayer graphite would exhibit a specific surface area close to 2700 m2/g, by comparing the total pore area of EG specimens in Table 2 to that of monolayer graphite, the number of graphene layers in a single particle of EG can be calculated [28]. If an interlayer spacing of 0.335 nm is assumed for bulk graphite, the average thickness of the EG specimens thus can be readily estimated [28]. Fig. 12 shows the estimated number of graphene layers and the thickness of EG particles. Now with knowing the thickness of EG particles and the bulk density of EG, one can calculate the specific surface area by using the definition of density being the ratio of mass to volume. For example for EG1 with a density of 0.0038 g/cc considering a thickness of 29 nm for the EG graphite thickness and a bulk density of 2.3 g/cc for graphite a specific surface area of 30 m^2/g is obtained by mass conservation law in a unit volume. The obtained surface area of 30 m^2/g from this calculation is close to the specific pore area of 31 m^2/g obtained from porosimetry. Therefore the pore area and specific surface area of EG specimens obtained in this work are verified to be valid. In other words the specific surface area from porosimetry measurements and pore volume from density measurements are consistent with the quantitative porous structure seen in the SEM images.

4. Model

The studies of dynamic properties of macromolecular chains in a random environment like porous media has been the interesting sub-

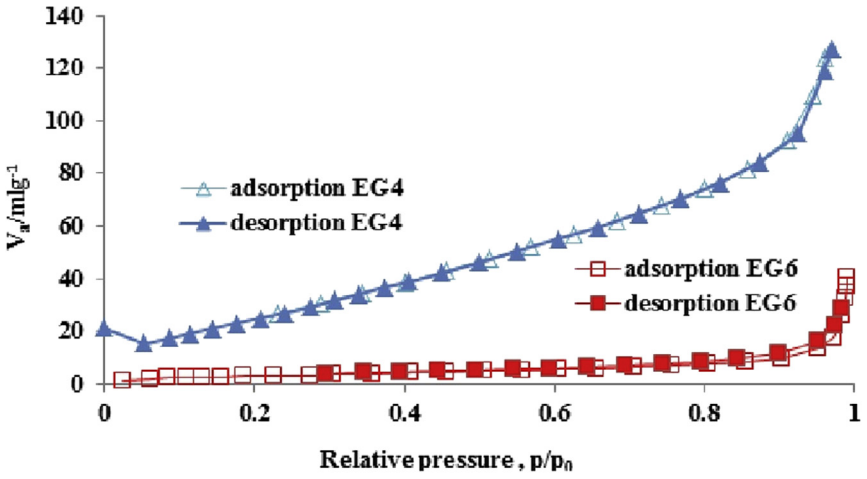

(a)

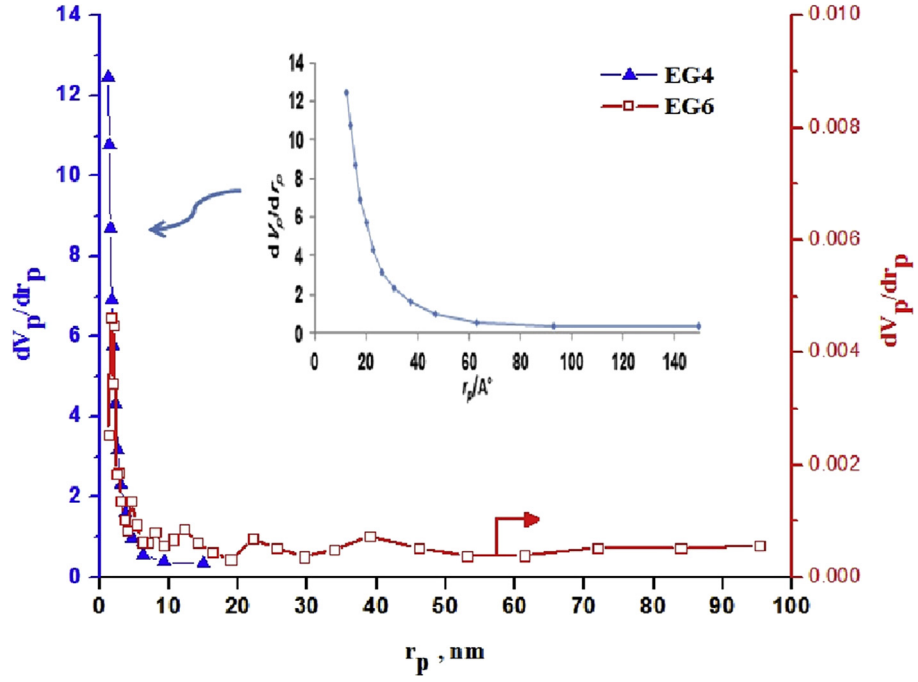

(b)

Fig. 9. (a) Adsorption/desorption isotherm, (b) dBJH plot of EG4 and EG6 by N_2 adsorption analysis.

Table 3
The pore volume and the surface area of EG4 and EG6 from nitrogen adsorption.

Sample	BET surface area (m^2/g)	pore volume (cm^3/g)
EG4 (900 °C, 50mesh)	37	0.17*
EG6 (900 °C, 200mesh)	11	0.06**

* For the pores in the range of 0–15nm.
** For the pores in the range of 0–100nm.

Table 4
The molecular weights of the silicone oils [38].

Viscosity (cSt)	100	350	1000
Average molecular weight (g/mol)	5970	13650	28000
Estimated radius of gyration (Å)	19	34	50

ject of many simulations studies [39, 40]. The reason is the practical importance of such systems, like polymer behavior in capillary electrophoresis, coating the surfaces, laminates, chromatography, colloidal stabilization etc. [41]. Monte Carlo (MC) simulation is one of the most important tools in the study of diffusion processes [42]. It is reported that the result of the MC method with a step length taken from an appropriate Gaussian distribution and, a constant diffusion coefficient, is the same as the exact result i.e. the result from the integration of the diffusion equation. The MC simulations have modeled the solid phase of the porous medium with certain porosity (p) by the set of clusters obtained via the random site percolation and the polymer by the freely jointed chains [43]. For instance, scaling relations such as between the diffusion constant D and polymer length N, $D \propto N^{-1}$, for polymer confined in homogeneous channels obtained from MC simulation are in good agreement with the theoretical prediction [41]. Baumgartner

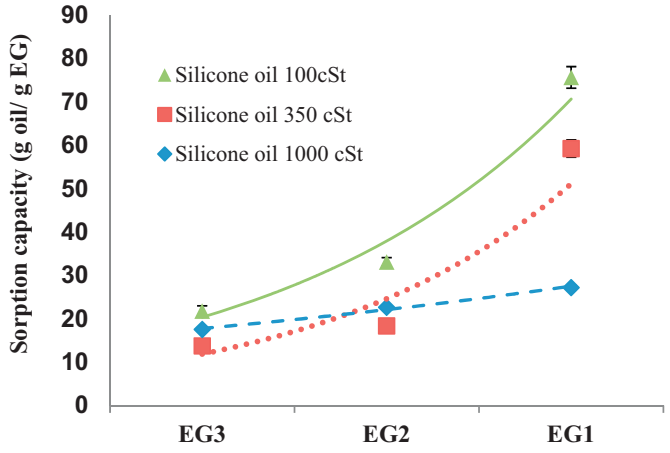

Fig. 10. The oil sorption capacities of EGs prepared at different exfoliation temperatures.

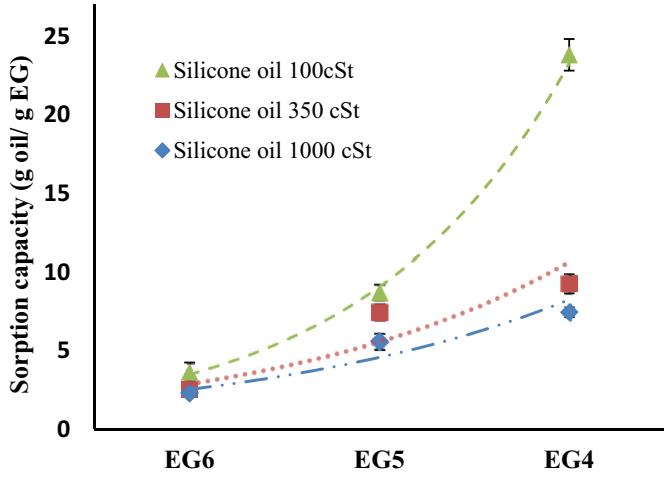

Fig. 11. The oil sorption capacities of EGs prepared from GICs with different average particle size.

Table 5
The percentage of filled pore volume of EG specimens by silicone oils.

Partial Oil filling (vol%)						
	EG1	EG2	EG3	EG4	EG5	EG6
Silicone oil 100 cSt	29.8	15.1	11.1	23.2	9.6	13.2
Silicone oil 350 cSt	23.3	8.4	7	7.3	14.2	14.6
Silicone oil 1000 cSt	10.7	10.3	8.9	7.2	14.9	20.8

et al [44] investigated dynamic properties of a polymer chain, which performs Brownian motion between randomly distributed impenetrable fixed obstacles by MC simulations. The mean square radius of gyration, diffusion constant D, and the longest relaxation time are functions of $((1-p)\sqrt{N})$, for all chain lengths N and porosities p above the percolation threshold. Sikorski et al [45] investigated how the density of obstacles changes the diffusion coefficient of star-branched polymer chains in porous media at two temperatures. They found that an increase in the density of obstacles strongly decreases the mobility of chains in both temperatures porosity. Sikorski [46] also simulated the changes of the diffusion constant D with the chain length N for all macromolecular architectures, put in the slit with the obstacles. The diffusion constant scales as N^{-a}, at least for linear and cyclic chains longer than N = 50. For linear chains, $D \sim N^{-1.68\pm0.04}$, while for rings the diffusion constant scales as $D \sim N^{-1.2\pm0.03}$. According to the results of MC simulations, we found a relationship between the sorption capacity of EG with its total pore area and molecular weight of silicone oils. Fig. 13 presents the linear dependence of sorption capacity of EG on the square root of molecular weight of the penetrating macromolecular chains.

Interestingly, the slopes of the extracted line equations in Fig. 13 are a function of the total pore area of EG (as shown in Fig. 14). So, we propose a new model as given in Eq. (1) for the dependence of sorption capacity of EG to its pore area and molecular weight of diffusing macromolecule. Furthermore, a critical value of about 25 m^2/g can be assigned which above that oil sorption capacity suddenly increases.

$$Sc = -A(p) \times \sqrt{M_w} + b \quad (1)$$

Where Sc is the sorption capacity of EG, b is a constant, M_w is molecular weight of silicone oil and A(p) is a coefficient as a function of pore area of EG. As shown in Fig. 14, A(p) is a function of pore area through the following equations (Eqs. (2) and (3)):

$$A(p) = d \times p + f \quad \text{for EG with pore area} \quad >25 \quad m^2/g \quad (2)$$

$$A(p) = g \times exp^{h \times p} \quad \text{for EG with pore area} \quad <25 \quad m^2/g \quad (3)$$

Where p is the pore area of EG and d, f, g and h are constant values. Eq. (3) gives the slope for EGs with low pore area prepared from GICs with smaller particle size. It is seen that the slope of sorption capacity equation tends to zero at very low pore area or porosity. This model can improve the design and synthesis methods of different EG types and EG composites for specific applications such as highly efficient sorbents for removal of oil products from water surface.

5. Conclusion

In this paper the microstructure of expanded graphite (EG) as an effective nanographite material for use in polymer composites was investigated. The influences of exfoliation temperature from 700 to 900 °C and the average particle size of GIC from 35 mesh to 200 mesh on the microstructure of the obtained EGs were studied. The EG specimens were characterized by mercury porosimetry, FTIR, bulk density, SEM and nitrogen adsorption/desorption. It was found from mercury porosimetry and nitrogen adsorption that the prepared EGs contain pores with sizes dominant in the range of 0.1–100 microns. With increasing GIC particle size and exfoliation temperature the exfoliation volume, pore volume and surface area of the prepared EG specimens were increased. However the effect of GIC particles size on these properties was stronger than the effect of exfoliation temperature. The sorption of silicone oil into EG galleries was discussed as a criterion for the macromolecular diffusion into EG and as a function of bulk density, total pore area and pore size distribution. It was found that with the increase of silicone oil molecular weight the sorption capacity decreases. Furthermore the pores were not fully filled with silicon oil suggesting that there are relatively closed pores in the EGs. The pore volume calculated from bulk density being much higher than the pore volume measured by mercury porosimetry supported the presence of closed cells. A critical value of about 25 m^2/g for the pore area was identified which above that oil sorption capacity suddenly increased. Empirical correlations between the structural characteristics of EG and the penetrated volume fraction of EG by silicone oils were observed. A new model was proposed to estimate the oil sorption capacity of EG as a function of oil molecular weight and EG pore area.

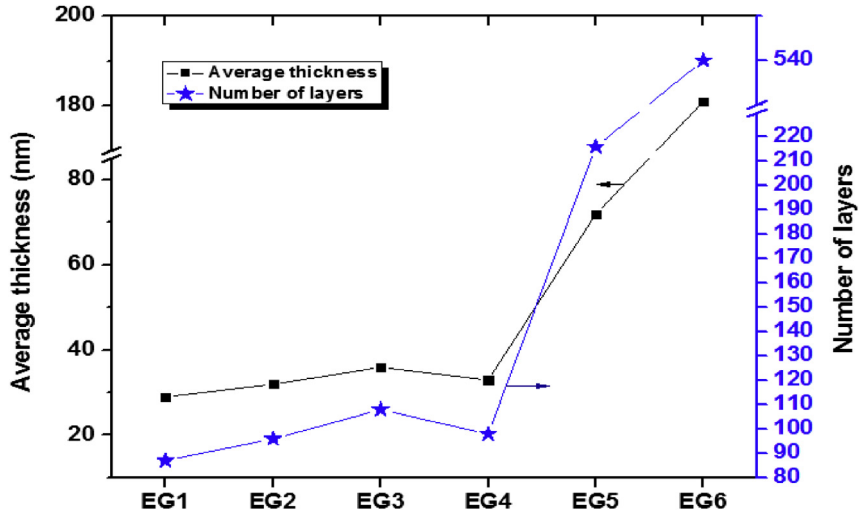

Fig. 12. The average thickness and the number of layers of EG specimens.

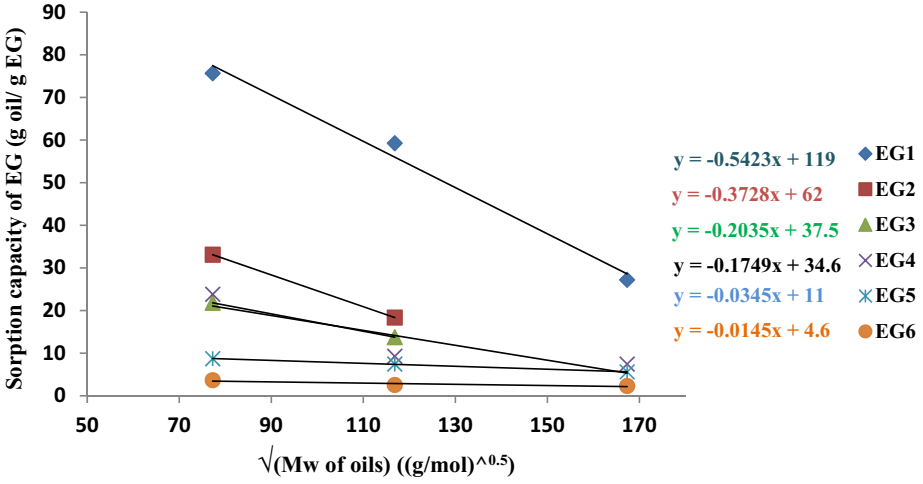

Fig. 13. The sorption capacity of EG as a function of the molecular weight of silicone oils. The trend line equations of EG types are given in the inset.

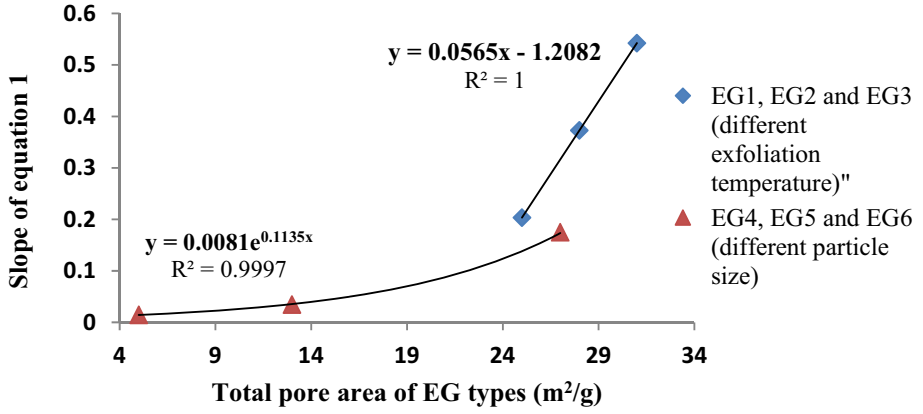

Fig. 14. The plot for the equation slope of sorption capacity of EG vs total pore area of EG.

Declarations

Author contribution statement

Ghodratollah Hashemi Motlagh: Conceived and designed the experiments; Analyzed and interpreted the data; Contributed reagents, materials, analysis tools or data; Wrote the paper.

Rahimeh Goudarzi: Conceived and designed the experiments; Performed the experiments; Analyzed and interpreted the data; Wrote the paper.

Funding statement

This research did not receive any specific grant from funding agencies in the public, commercial, or not-for-profit sectors.

Competing interest statement

The authors declare no conflict of interest.

Additional information

No additional information is available for this paper.

References

[1] R. Sengupta, M. Bhattacharya, S. Bandyopadhyay, A.K. Bhowmick, Progress in Polymer Science A review on the mechanical and electrical properties of graphite and modified graphite reinforced polymer composites, Prog. Polym. Sci. 36 (2011) 638–670.
[2] M. Jalili, H. Ghanbari, S. Moemen Bellah, R. Malekfar, High-quality liquid phase-pulsed laser ablation graphene synthesis by flexible graphite exfoliation, J. Mater. Sci. Technol. 35 (2019) 292–299.
[3] T. Liu, R. Zhang, X. Zhang, K. Liu, Y. Liu, P. Ya, One-step room-temperature preparation of expanded graphite, Carbon N. Y. 119 (2017) 544–547.
[4] A.E. Teplykh, S.G. Bogdanov, Y.A. Dorofeev, A.N. Pirogov, Y.N. Skryabin, V.G. Makotchenko, A.S. Nazarov, V.E. Fedorov, Structural state of expanded graphite prepared from intercalation compounds, Crystallogr. Rep. 51 (2006) 62–66.
[5] M. Toyoda, M. Inagaki, Heavy oil sorption using exfoliated graphite: new application of exfoliated graphite to protect heavy oil pollution, Carbon N. Y. 38 (2000) 199–210.
[6] I.M. Afanasov, O.I. Lebedev, B.A. Kolozhvary, A.V. Smirnov, G. van Tendeloo, Nickel/Carbon composite materials based on expanded graphite, N. Carbon Mater. 26 (2011) 335–340.
[7] Y.L. Zhong, T.M. Swager, Enhanced electrochemical expansion of graphite for in situ electrochemical functionalization, J. Am. Chem. Soc. 134 (2012) 17896–17899.
[8] L. Yu, Y.H. Zhang, W.S. Tong, Hierarchical composites of conductivity controllable polyaniline layers on the exfoliated graphite for dielectric application, Compos. A 43 (2012) 2039–2045.
[9] G. Katsukis, J. Malig, C. Schulz-Drost, S. Leubner, N. Jux, D.M. Guldi, Toward combining graphene and QDs: assembling CdTe QDs to exfoliated graphite and nanographene in water, ACS Nano 6 (2012) 1915–1924.
[10] M. Inagaki, M. Toyoda, N. Iwashita, Sorption of Viscous Organics by Macroporous Carbons, 2008.
[11] A. Yasmin, J. Luo, I.M. Daniel, Processing of expanded graphite reinforced polymer nanocomposites, Compos. Sci. Technol. 66 (2006) 1179–1186.
[12] M. Bonnissel, L. Luo, D. Tondeur, Compacted exfoliated natural graphite as heat conduction medium, Carbon N. Y. 39 (2001) 2151–2161.
[13] I.M. Afanasov, O.N. Shornikova, I.I. Vlasov, E.V. Kogan, A.N. Seleznev, V.V. Avdeev, Porous carbon materials based on exfoliated graphite, Inorg. Mater. 45 (2009) 171–175.
[14] I.M. Afanasov, D.V. Savchenko, S.G. Ionov, D.A. Rusakov, A.N. Seleznev, V.V. Avdeev, Thermal conductivity and mechanical properties of expanded graphite, Inorg. Mater. 45 (2009) 486–490.
[15] M. Inagaki, N. Iwashita, E. Kouno, Potential change with intercalation sulfuric acid into graphite, Carbon N. Y. 28 (1990) 49–55.
[16] G. Hristea, P. Budrugeac, Characterization of exfoliated graphite for heavy oil sorption, J. Therm. Anal. Calorim. 91 (2008) 817–823.
[17] S. Tao, S. Wei, Y. Yulan, Characterization of expanded graphite microstructure and fabrication of composite phase-change material for energy storage, J. Mater. Civ. Eng. 27 (2015), 04014156.
[18] V. Sridhar, J. Jeon, I. Oh, Synthesis of graphene nano-sheets using eco-friendly chemicals and microwave radiation, Carbon N. Y. 48 (2010) 2953–2957.
[19] S.R. Dhakate, R.B. Mathur, S. Sharma, M. Borah, T.L. Dhami, Influence of expanded graphite particle size on the properties of composite bipolar plates for fuel cell application, Energy Fuel. 23 (2009) 934–941.
[20] G. Zheng, J. Wu, W. Wang, C. Pan, Characterizations of expanded graphite/polymer composites prepared by in situ polymerization, Carbon N. Y. 42 (2004) 2839–2847.
[21] L. Wang, L. Zhang, M. Tian, Effect of expanded graphite (EG) dispersion on the mechanical and tribological properties of nitrile rubber/EG composites, Wear 276–277 (2012) 85–93.
[22] M. Murariu, A.L. Dechief, L. Bonnaud, Y. Paint, A. Gallos, G. Fontaine, S. Bourbigot, P. Dubois, The production and properties of polylactide composites filled with expanded graphite, Polym. Degrad. Stab. 95 (2010) 889–900.
[23] W. Jia, R. Tchoudakov, M. Narkis, Performance of expanded graphite and expanded milled-graphite fillers in thermosetting resins, Polym. Compos. (2005) 526–533.
[24] R. Goudarzi, G.H. Motlagh, M. Elhamnia, S. Motahari, Graphite nanosheet as low shrinkage additive, curing accelerator, and conducting filler for unsaturated polyester resin, Polym. Plast. Technol. Eng. 55 (2016) 1231–1239.
[25] B. Tryba, R.J. Kalenczuk, F. Kang, M. Inagaki, A. Morawski, Studies of exfoliated graphite (eg) for heavy oil sorption, Md. CrWyst. Lty. Cryt. 340 (2000) 113–119.
[26] M. Inagakl, H. Konno, M. Toyoda, K. Moriya, Sorption and recovery of heavy oils by using exfoliated graphite Part II : recovery of heavy oil and recycling of exfoliated graphite 128 (2000) 213–218.
[27] N.B. Hoang, T.T. Nguyen, T.S. Nguyen, T. Phuong, Q. Bui, L.G. Bach, N.D. Duc, The application of expanded graphite fabricated by microwave method to eliminate organic dyes in aqueous solution, Cogent Eng. 6 (2019) 1–13.
[28] G. Chen, W. Weng, D. Wu, C. Wu, J. Lu, P. Wang, X. Chen, Preparation and characterization of graphite nanosheets from ultrasonic powdering technique, Carbon N. Y. 42 (2004) 753–759.
[29] C.P. Herrero, R. Ramirez, Diffusion of hydrogen in graphite: a molecular dynamics simulation, J. Phys. D-Applied Phys. 43 (2010) 255402.
[30] A. Celzard, J. Mareche, Permeability and formation factor in compressed expanded graphite, J. Phys. Condens. Matter 13 (2001) 4387–4403.
[31] N. Gulnura, K. Kenes, O. Yerdos, Preparation of expanded graphite using a thermal method, IOP Conf. Ser. Mater. Sci. Eng. 323 (2018).
[32] L. Wang, X. Fu, E. Chang, H. Wu, K. Zhang, X. Lei, R. Zhang, X. Qi, Y. Yang, Preparation and its adsorptive property of modified expanded graphite nanomaterials, J. Chem. 2014 (2014) 1–5.
[33] W.C. Hung, K.H. Wu, D.Y. Lyu, K.F. Cheng, W.C. Huang, Preparation and characterization of expanded graphite/metal oxides for antimicrobial application, Mater. Sci. Eng. C 75 (2017) 1019–1025.
[34] G. Mariz, D.O. Barra, A.D.A. Lucas, Chapter7. Expanded graphite as a multifunctional filler for polymer nanocomposites. Multi-Functionality of Polymer Composites, Elsevier Inc., 2015.
[35] H. Hua, Y. Wang, Y. Wang, S. Ruan, C. Zeng, T. Zhang, M. Zhu, Preparation of Expanded Graphite Using Recycling Graphite Rods by Microwave Irradiation, 2013, pp. 2356–2360.
[36] L.M. Anovitz, D.R. Cole, Characterization and analysis of porosity and pore structures, Rev. Mineral. Geochem. 80 (2015) 61–164.
[37] I. Evbuomwan, The Structural Characterisation of Porous media for Use as Model Reservoir Rocks, Adsorbents and Catalysts, University of Bath, 2009.
[38] Poly(dimethylsiloxane), in: A.C.M. Kuo, J.E. Mark (Eds.), Polym. Data Handbook, 1999, pp. 411–435.
[39] L. Plante, F. Cucinotta, Theory and Applications of Monte Carlo Simulations, Intech, 2013.
[40] C.-H. Yeh, B. Schmitt, B. Le, L. Denis, L. Jing, P. Ching, Diffusion microscopist simulator: a general Monte Carlo simulation system for diffusion magnetic resonance imaging, PLoS One 8 (2013) e76626.
[41] Y.-C. Chen, Y.-L. Zhou, C. Wang, Monte Carlo simulation on the diffusion of polymer in narrow periodical channels, Int. J. Mod. Phys. B 31 (2017) 1750144.
[42] M. Ghiass, An introduction to the Monte Carlo simulation methods, Polymer 4 (2014) 67–77.
[43] V. Ruiz Barlett, M. Hoyuelos, H.O. Martin, Monte Carlo simulation with fixed steplength for diffusion processes in nonhomogeneous media, J. Comput. Phys. 239 (2013) 51–56.
[44] A. Baumgartner, M. Muthukumar, A trapped polymer chain in random porous media, J. Chem. Phys. 87 (1987) 3082–3090.
[45] A. Sikorski, P. Adamczyk, Diffusion of polymer chains in porous media . A Monte Carlo study, Polymer 51 (2010) 581–586.
[46] A. Sikorski, P. Romiszowski, The computer simulations of polymer dynamics in porous media, Rheol. Acta 45 (2006) 583–589.